Supporting Information for

The Product of NH_3 loss from Gas Phase Protonated Tyrosine

Griffin Loebsack,[a,b,c‡] Neville J. A. Coughlan,[a,b‡] Lara van Tetering,[d,e] Yuting Li,[a,b] Nour Mashmoushi,[a,b] Yiming Xiao,[a] Mircea Guna,[f] Bradley B. Schneider,[f] J. C. Yves Le Blanc,[f] Jonathan Martens,[d,e] and W. Scott Hopkins[a,b,c*]

[a] Department of Chemistry, University of Waterloo, 200 University Avenue West, Waterloo, Ontario, N2L 3G1, Canada.

[b] Waterloo Institute of Nanotechnology, University of Waterloo, 200 University Avenue West, Waterloo, Ontario, N2L 3G1, Canada

[c] WaterFEL Free Electron Laser Laboratory, University of Waterloo, 200 University Avenue West, Waterloo, Ontario, N2L 3G1, Canada.

[d] HFML-FELIX, Toernooiveld 7, 6525 ED Nijmegen, the Netherlands

[e]Institute for Molecules and Materials, Radboud University, Heyendaalseweg 135, 6525 AJ Nijmegen, the Netherlands

[f]SCIEX, Four Valley Drive, Concord, Ontario, L4K V48, Canada

Table of Contents

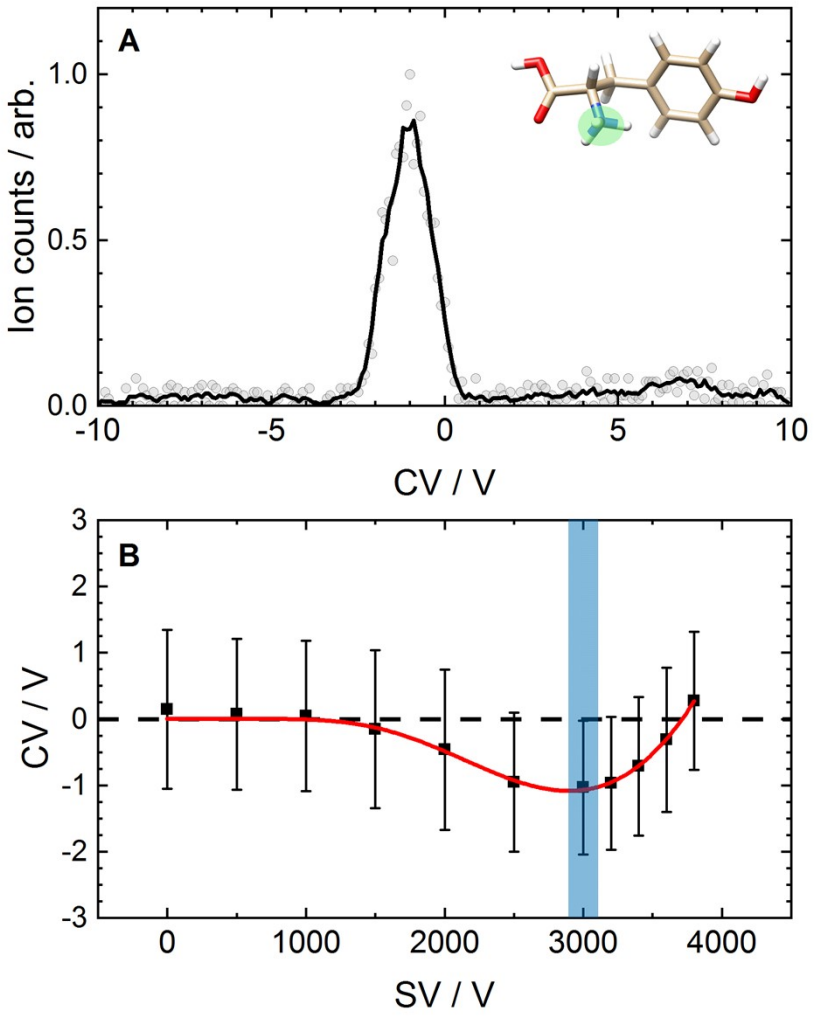

Figure S1. (**A**) The ionogram plot for $[Tyr + H]^+$ electrosprayed from 50:50 MeOH:H_2O with 0.5% formic acid solution in and N_2 environment at SV=3000V and (**B**) the dispersion plot for $[Tyr + H]^+$ in N_2 gas with the selected SV for A shown in blue. The error bars depict the full width half maximum (FWHM) of the DMS ionogram peak.

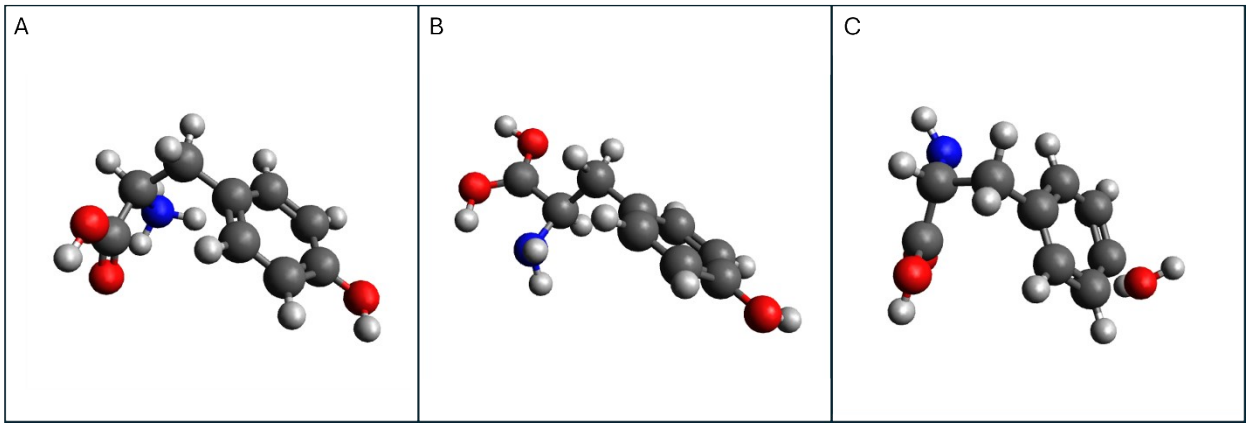

Figure S2. The geometries for the (**A**) N-protonated, (**B**) O-protonated, and (**C**) hydroxy O-protonated prototropic isomers of $[Tyr + H]^+$ optimized at the ωB97X-D3BJ / def2-TZVPP level of theory.

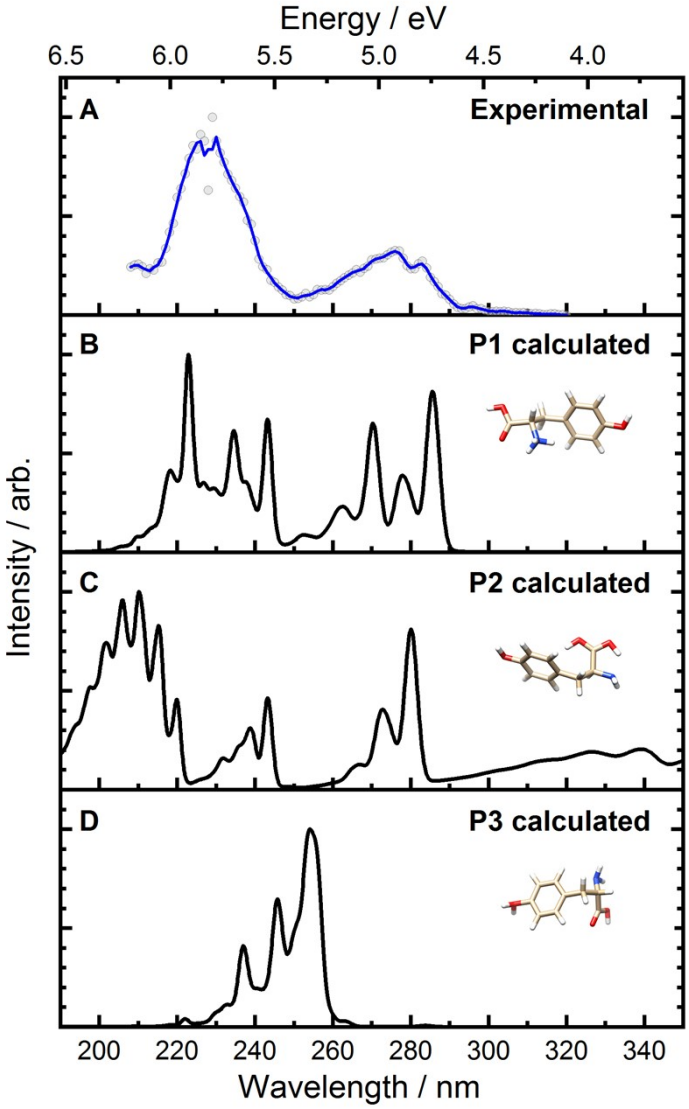

Figure S3. (**A**) The experimental UVPD action spectrum of $[Tyr + H]^+$, and the thermally averaged (T = 298 K) calculated VG|FC vibronic spectra for (**B**) N-protonated, (**C**) O-protonated, and (**D**) hydroxy O-protonated prototropic isomers of $[Tyr + H]^+$. Calculations were conducted at the ωB97X-D3BJ / def2-TZVPP level of theory. A spectra shift of –0.3 eV was applied for the VG|FC predictions.

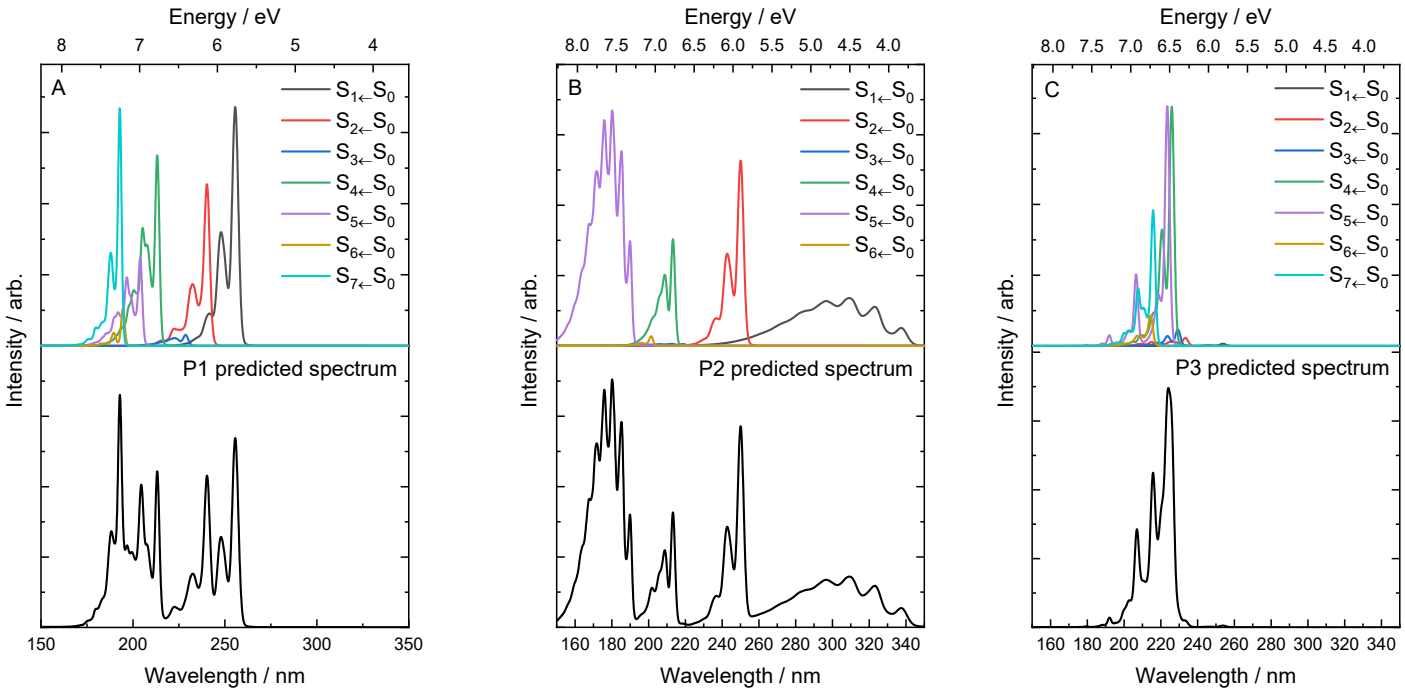

Figure S4. (**A**) The calculated spectra for (**A**) N-protonated, (**C**) O-protonated, and (**D**) hydroxy O-protonated prototropic isomers of $[Tyr + H]^+$ from the ground electronic state S_0 to S_n using the VG|FC approximation and the sum of the S_1 to S_7 transitions (lower).

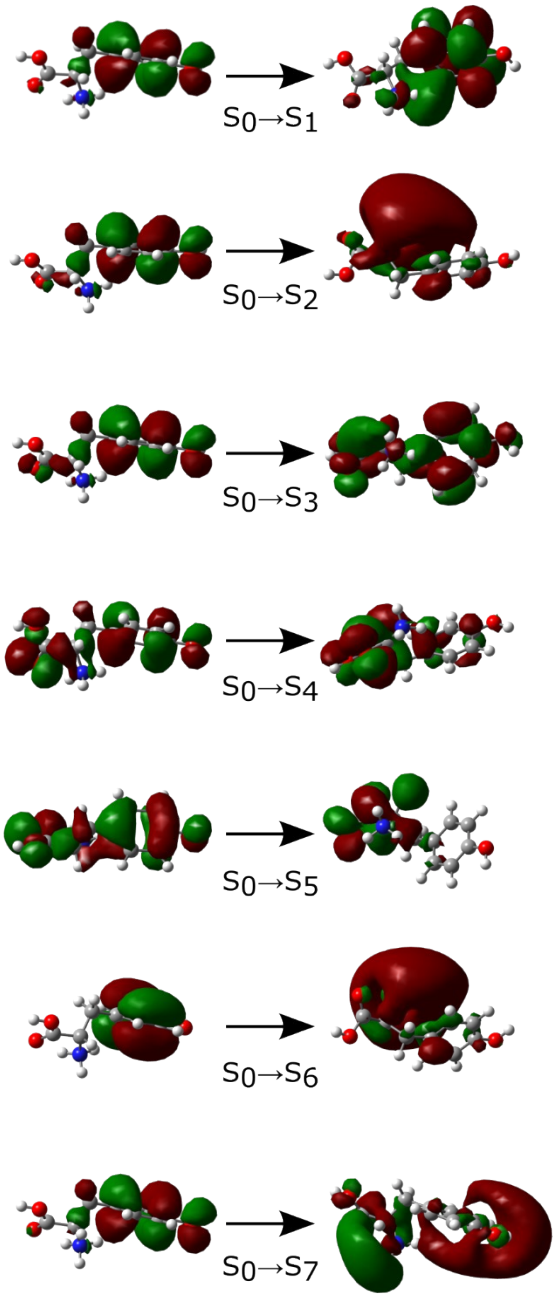

Figure S5. The calculated transition orbitals (HOTO-LUTO) associated with $S_n \rightarrow S_0$ transitions for the N-protonated protoropic isomer of $[Tyr + H]^+$.

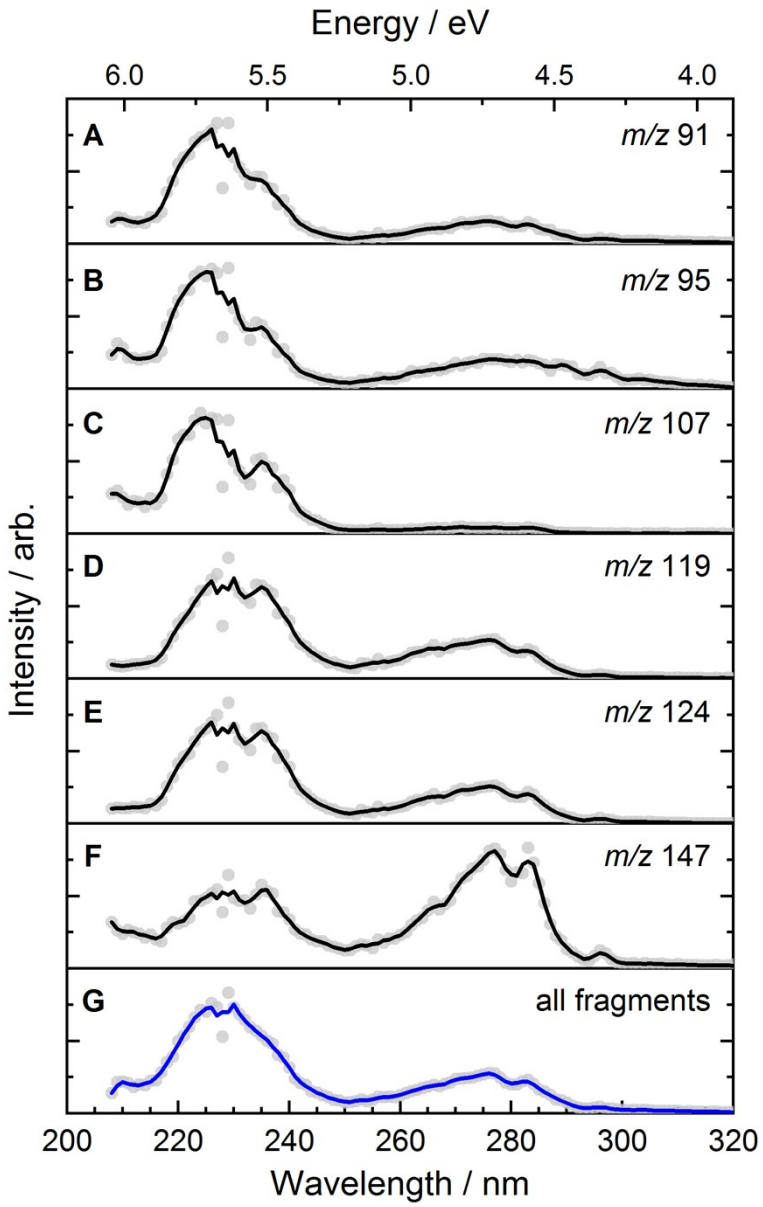

Figure S6. The UVPD action spectra for $[Tyr + H]^+$ as monitored in product channels (**A**) m/z 91, (**B**) m/z 95, (**C**) m/z 107, (**D**) m/z 119, (**E**) m/z 124, (**F**) m/z 147, (**G**) sum of fragments.

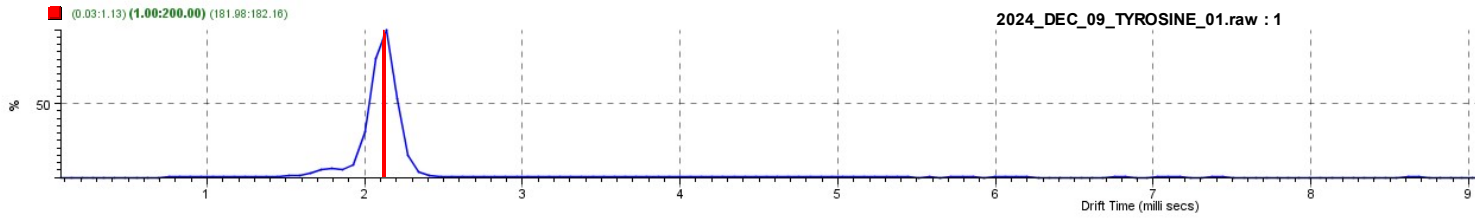

A

B

Figure S7. Mobiligrams of (**A**) $[Tyr + H]^+$ (m/z 182) and (**B**) $[Tyr - NH_3 + H]^+$ (m/z 165) measured using a Waters Synapt G2-Si HDMS mass spectrometer equipped with a TWIMS cell.

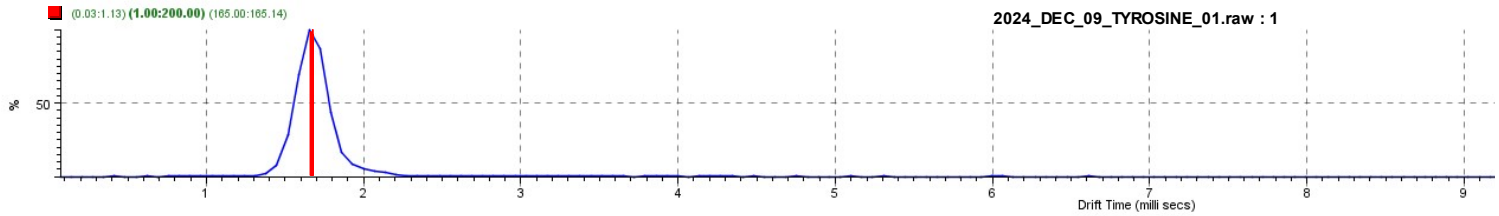

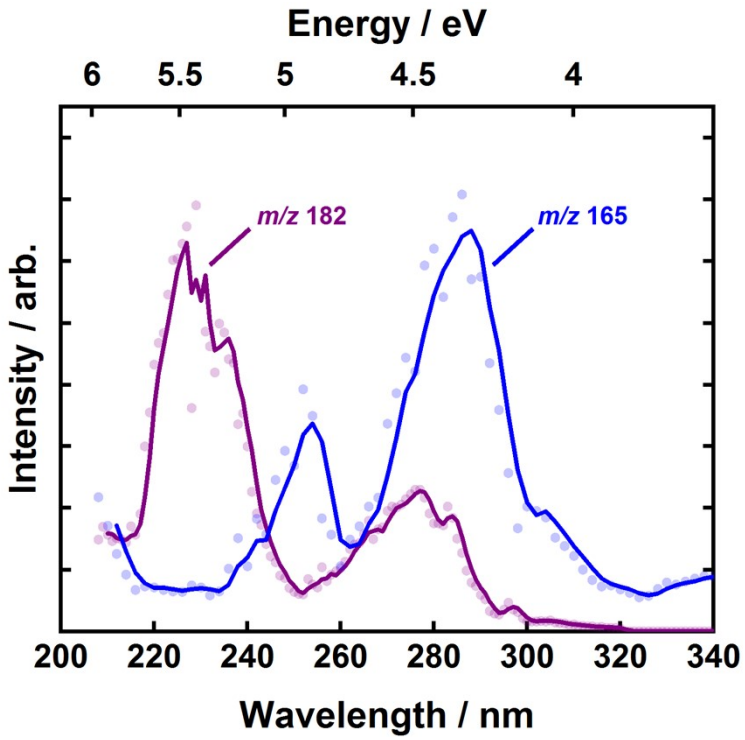

Figure S8. The UVPD action spectra of $[Tyr + H]^+$ (m/z 165) and $[Tyr - NH_3 + H]^+$ (m/z 182). $[Tyr - NH_3 + H]^+$ was generated via CID in Q2, then trapped in Q3 for laser interrogation.

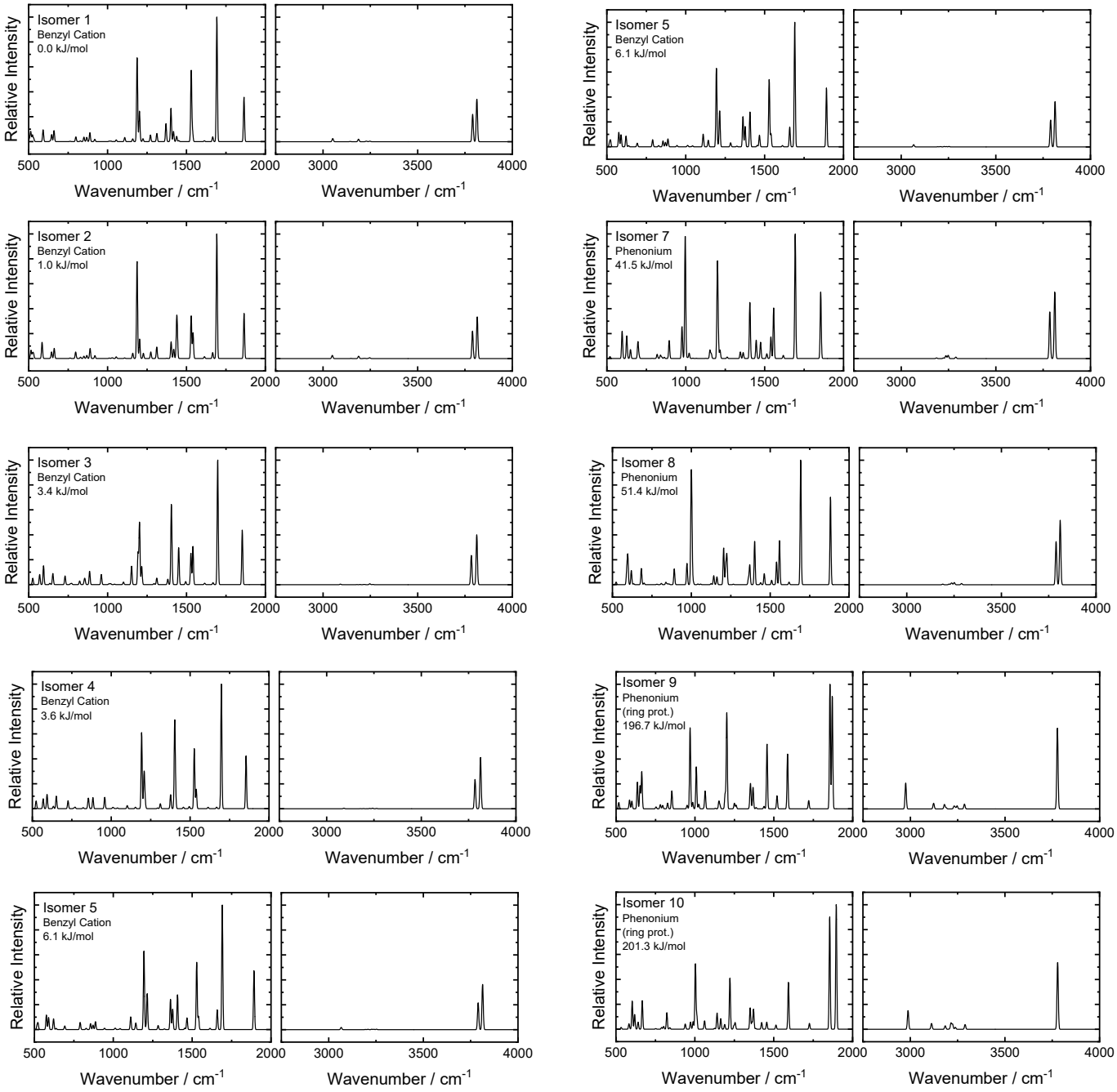

Figure S9. The calculated harmonic vibronic spectra of the benzyl cation and phenonium isomers of $[Tyr - NH_3 + H]^+$ calculated at the ωB97X-D3BJ / def2-TZVPP level of theory.

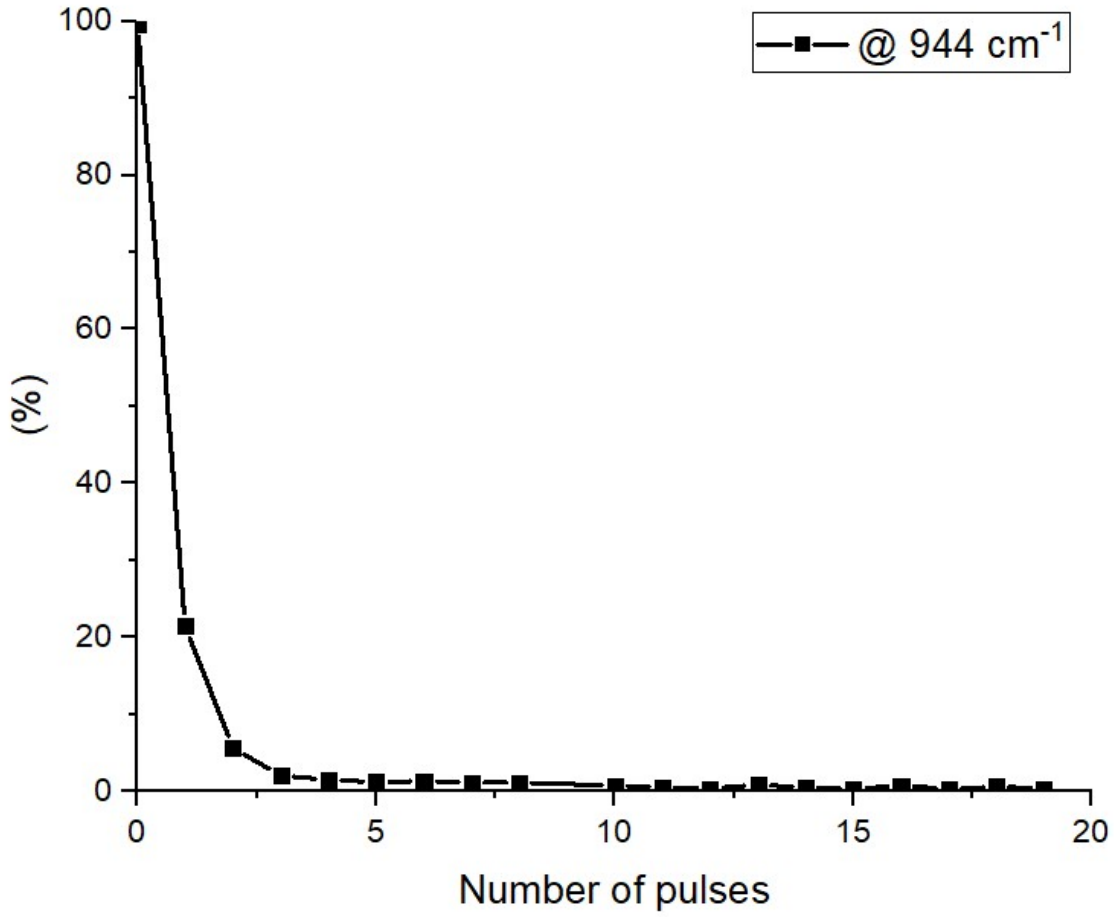

Figure S10. IRIS isomer population analysis curve with increasing laser pulses performed at 944 cm^{-1}.